(pH 7.6), 1 mM EDTA, and 1 mM phenylmethylsulfonyl fluoride. After centrifugation, the supernatant was added to an equal volume of 90% (w/v) ammonium sulfate and left on ice for 30 min. The samples were centrifuged, and the protein pellets were resuspended in 0.5 ml of 10 mM tris (pH 7.6) with 1 mM EDTA. The relative concentration of each fusion protein was determined by SDS–polyacrylamide gel electrophoresis (SDS-PAGE) under reducing conditions with Coomassie blue staining and laser-scanning densitometry; all sample volumes were adjusted to give the same concentration of protein. The hGHbp was coupled to Affi-Gel 15 (5 ml), (Bio-Rad) according to the manufacturer's instructions and made up to a total volume of 10 ml in 10 mM tris (pH 7.6), and 1 mM EDTA. The affinity matrix (40 μl) was incubated with 100 μl (~1 μg) of hGH-AP fusion protein for 2 hours with slow tumbling at room temperature. The supernatant was removed, and the beads were washed twice in 1 ml of 10 mM tris (pH 7.6) with 1 mM EDTA and once in 0.5 ml of 20 mM tris (pH 8.6) with 100 mM NaCl. The H64A subtilisin variant (100 μl of 500 nM) was added, and the beads were incubated with tumbling for 10 min at room temperature. The supernatant was removed and assayed for AP activity by incubating a sample (20 μl) with 180 μl of 6.6 mM *p*-nitrophenyl phosphate (Sigma) in 0.6 M tris (pH 8.2) for 2 hours at room temperature with shaking and measuring the absorbance change at 405 nm caused by production of *p*-nitroaniline. The amount of AP released with no protease added was also measured.

17. For NH_2-terminal sequence analysis, AP cleavage products were isolated essentially as described (*16*), but 100 μl of Affi-Gel slurry and 200 μl of fusion protein were used for each sample. Also, the protease concentration was increased to 2 μM in a volume of 50 μl, and the cleavage reaction proceeded for 1 hour. The resulting AP digestion products were electroblotted onto polyvinylidene difluoride membrane [P. Matsudaira, *J. Biol. Chem.* **262**, 10035 (1987)], and the NH_2-termini were sequenced with a protein sequencer (Applied Biosystems 473 or 477).
18. P. Carter, L. Abrahmsen, J. A. Wells, *Biochemistry* **30**, 6142 (1991). Cleavage of the FAHF-*p*-nitroanilide substrate by either the wild-type or the H64A variant does not produce a burst of production of *p*-nitroaniline, which indicates that acylation is rate limiting. Furthermore, the k_{cat} for cleavage of a FAQF-thiobenzyl ester substrate (where deacylation is presumed to be rate limiting) by the H64A variant is 1×10^{-2} s^{-1}, whereas the k_{cat} for cleavage of an FAHF-*p*-nitroanilide substrate (where His-assisted acylation is rate limiting) is 2×10^{-2} s^{-1}. This suggests that His-assisted catalysis is critical for acylation but not as important for deacylation.
19. K. Nagai and H. C. Thogersen, *Nature* **309**, 810 (1984).
20. K. Cho *et al.*, *Biochemistry* **23**, 644 (1984); R. Lottenberg, U. Christensen; C. M. Jackson, L. Coleman, *Methods Enzymol.* **80**, 341 (1981).
21. S. Kawabata *et al.*, *Eur. J. Biochem.* **172**, 17 (1988).
22. C. Debouck, *AIDS Res. Human Retroviruses* **8**, 153 (1992).
23. S. C. B. Yan, B. W. Grinnell, F. Wold, *Trends Biochem. Sci.* **14**, 264 (1989).
24. The phagemid phGH-LIB-g3 was derived from phGHam-g3 (*4*). Site-directed mutagenesis of phGHam-g3 with the oligonucleotide 5′-AGCTGTGGCTTCGGGCCCGCCGCCGCGTCGACTGGCGGTGGCTCT-3′ resulted in the amber stop codon being replaced by a short Apa I–Sal I cassette. The wild-type hGH gene was replaced with the gene for a tight-binding hGH molecule by exchange of an Apa I–Hinc II fragment from the phagemid pDM0390 (*10*). The short Apa I–Sal I cassette was excised and replaced by a longer cassette constructed from the oligonucleotides 5′-CTAATGATAATGAATTAATTGATAATGATAATG-3′ and 5′-TCGACATTATCATTATCAATTAATTCATTATCATTAGGGCC-3′ so that the Sal I site was no longer at the end of a fragment and could be cut more efficiently. The cassette contains eight stop codons and introduces a frame-shift mutation between hGH and gene III that ensures that when library cassettes are introduced only plasmids containing a randomized substrate insert will be propagated as hGH-displaying phage.
25. W. J. Dower, J. F. Miller, C. W. Ragsdale, *Nucleic Acids Res.* **16**, 6127 (1988).
26. F. Sanger, S. Nicklen, A. R. Coulson, *Proc. Natl. Acad. Sci. U.S.A.* **74**, 5463 (1977).
27. C. S. Wright, R. A. Alden, J. Kraut, *Nature* **221**, 235 (1969).
28. Y. Mitsui, Y. Satow, Y. Watanabe, Y. Iitaka, *J. Mol. Biol.* **131**, 697 (1979).
29. We thank S. Bass for supplying hGH–gene III and some preliminary substrate phagemid vectors, W. Henzel and S. Wong for help with protein sequencing, the oligonucleotide group at Genentech for supplying synthetic DNA, R. Lazarus and J. Seymour for providing factor X_a and for advice on its use, C. Craik for supplying HIV protease, W. Anstine for graphics, and M. Zoller for comments and critical reading of the manuscript.

28 December 1992; accepted 9 March 1993

Structure of the Retinoid X Receptor α DNA Binding Domain: A Helix Required for Homodimeric DNA Binding

Min S. Lee,* Steven A. Kliewer, Joan Provencal, Peter E. Wright,† Ronald M. Evans†

The three-dimensional solution structure of the DNA binding domain (DBD) of the retinoid X receptor α (RXRα) was determined by nuclear magnetic resonance spectroscopy. The two zinc fingers of the RXR DBD fold to form a single structural domain that consists of two perpendicularly oriented helices and that resembles the corresponding regions of the glucocorticoid and estrogen receptors (GR and ER, respectively). However, in contrast to the DBDs of the GR and ER, the RXR DBD contains an additional helix immediately after the second zinc finger. This third helix mediates both protein-protein and protein-DNA interactions required for cooperative, dimeric binding of the RXR DBD to DNA. Identification of the third helix in the RXR DBD thus defines a structural feature required for selective dimerization of the RXR on hormone response elements composed of half-sites (5′-AGGTCA-3′) arranged as tandem repeats.

The mechanisms by which transcription factors bind to regulatory sequences and control expression of target genes is a central problem in eukaryotic molecular biology. Members of the nuclear hormone receptor superfamily contain a highly conserved region of ~70 amino acids, including two zinc fingers, that is required for specific binding to DNA sequences termed hormone response elements (HREs) (*1*). Typically, members of the family bind as dimers to HREs composed of two copies of a six-nucleotide motif, termed half-sites. A subset of the nuclear receptors, including the GR and ER, bind as homodimers to HRE half-sites oriented as inverted repeats (*1*). In contrast, other members of the nuclear receptor family, including the peroxisome proliferator–activated receptor (PPAR), vitamin D receptor (VDR), thyroid hormone receptor (TR), and retinoic acid receptor (RAR), preferentially bind and activate through HREs composed of half-sites arranged as direct repeats (DRs), with specificity conferred by both the half-site sequence and the number of nucleotides separating the two half-sites (*2*). Instead of binding as homodimers, these receptors form heterodimers with the RXR that bind with high affinity to target DNA (*3*, *4*). In addition to its role in heterodimeric complexes, the RXR also forms a homodimer that activates in response to 9-*cis* retinoic acid through HREs composed of DRs (*5*, *6*).

To determine the structural features of the RXR that promote binding to tandem repeat HREs, we expressed a 94-residue peptide (Fig. 1) that comprised the DBD of RXRα in *Escherichia coli* and purified it to near homogeneity (*7*). In gel mobility-shift assays (*8*), the RXR DBD peptide bound weakly to an oligonucleotide containing a single AGGTCA half-site (Fig. 2A). In contrast, the RXR DBD bound cooperatively to an oligonucleotide that contained two half-sites oriented as direct repeats, which indicates the presence of a dimerization signal in the DBD (Fig. 2A). The isolated RXR DBD retained the binding specificity of the full-length RXR protein (*6*), binding preferentially as a homodimer to a direct repeat of AGGTCA with a single nucleotide spacer relative to the other spacing options (Fig. 2B).

M. S. Lee and P. E. Wright, Department of Molecular Biology, The Scripps Research Institute, La Jolla, CA 92037.
S. A. Kliewer, J. Provencal, R. M. Evans, Howard Hughes Medical Institute, The Salk Institute for Biological Studies, La Jolla, CA 92037.

*Present address: Molecumetics Institute, 2023 120th Avenue, N.E., Suite 400, Bellevue, WA 98005.
†To whom correspondence should be addressed.

Nuclear magnetic resonance (NMR) studies of the 94-residue RXR DBD were performed. Like the DBDs of the GR, ER, and RAR (9–11), the RXR DBD was stable only within a limited range of temperature (<27°C) and pH (>6.5) (12). Sequence-specific resonance assignments were made by standard methods from homonuclear two-dimensional (2D) spectra and heteronuclear 2D and 3D spectra obtained from uniformly ^{15}N-labeled protein (13). Elements of regular secondary structure were identified on the basis of patterns of nuclear Overhauser effect (NOE) connectivities. They include a short stretch of antiparallel β-sheet (involving residues Cys^{135}, Ala^{136}, Ser^{151}, and Cys^{152}), regions of extended conformation, and three α-helical regions. All three helices were characterized by sequential NH–NH NOEs and extensive networks of medium-range NOE connectivities. The presence of the third helix was unexpected because it was not observed in either x-ray crystallographic analysis of the GR (14) or NMR studies of the GR (9), ER (10), and RARβ (11). No medium- or long-range NOEs were observed for residues beyond the third helix or in the NH_2-terminal region preceding the first zinc binding domain. These regions are largely disordered (15), and structure calculations were therefore limited to an 81-residue core (Ile^{134} to Asp^{214}). A total of 593 distance constraints derived from NOEs were used for structure determination (16), including 197 intraresidue, 155 sequential, 82 medium-range, and 159 long-range NOEs.

A family of 310 structures was calculated with the distance geometry program DISGEO (17, 18). From the initial family of distance geometry structures, 119 structures were subjected to an additional 4D refinement procedure. The 58 distance geometry structures with the lowest residual error were then used as starting structures for restrained molecular dynamics (rMD) calculations (19) with the AMBER all-atom force field (20). The conformation of the 81-residue DBD of the RXR is well defined by the NOE constraints and zinc coordination, except for the metal binding loops. The best 15 structures have a mean AMBER energy of −1154 kcal/mol and a mean NMR constraint violation energy of 11.1 kcal/mol. There are only 6.9 constraint violations larger than 0.1 Å per structure, on average, with a maximum violation of 0.46 Å. The rMD structures clearly show the presence of three α helices with characteristic φ, ψ torsion angles and CO_i–NH_{i+4} hydrogen bonds. The average root-mean-square (rms) deviation from the mean is 2.6 Å for backbone heavy atoms of residues 134 to 214 in the family of 15 structures. The average backbone rms deviation from the mean for a superposition of the helical regions is 1.04 Å. When the structures are superimposed to give a best fit for backbone heavy atoms for helix 1, helix 2, and helix 3 independently, the average backbone rms deviations from the mean are 0.37, 0.28, and 0.43 Å, respectively. Although the local backbone structure of helix 3 is very well defined, some disorder is apparent in the packing of this helix against helices 1 and 2.

The family of structures that result from rMD refinement is shown in Fig. 3, together with a backbone representation of the structure with lowest residual constraint violations. The helices are well defined, with considerable disorder in the two zinc binding domains. The first zinc binding site consists of residues Cys^{135} to Cys^{155}, with the last cysteine ligand situated near the NH_2-terminus of the first helix (Glu^{153} to Lys^{165}). The second zinc binding domain encompasses Cys^{171} to Cys^{190}. Helix 2 extends from Tyr^{189} to Gly^{199} and is packed against helix 1 so that the two helices cross at an angle of ~90°. Helix 3, which packs against helix 1 and the tip of the first zinc binding domain, is formed by residues Arg^{202} to Arg^{209}. It is separated from helix 2 by a distinct bend in the backbone at the invariant Gly-Met sequence. The molecule contains an extensive hydrophobic core formed by the side chains of Phe^{158}, Phe^{159}, Val^{163}, Leu^{167}, Tyr^{169}, Tyr^{189}, Tyr^{192}, and Leu^{196}, all of which are in or near helices 1 and 2. Val^{205} on helix 3 also forms part of this hydrophobic core, making close contacts with the side chains of Phe^{159} and Val^{163}. There may be additional stabilizing interactions between oppositely charged residues on helices 1 and 3 that are in close proximity in the NMR structures. The overall fold of the RXR DBD is similar to that of the GR (9, 14) and ER (10) DBDs, except that the RXR domain contains an additional helix (helix 3).

To determine whether the third helix functions in the binding of the RXRα DBD to its cognate HRE, we generated truncation derivatives of RXR DBD 130–223 (21) and tested them in a gel mobility-shift assay. An RXR DBD construct truncated at the COOH-terminal end of the third helix (RXR DBD 130–209) retains the ability to

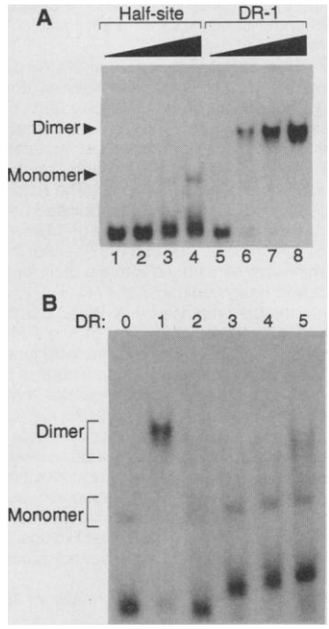

Fig. 2. The RXR DBD binds cooperatively to a DR-1 HRE. (**A**) Gel mobility-shift assays employed progressively increasing amounts of RXR DBD 130–223 and ^{32}P-labeled oligonucleotides encoding either an intact DR-1 HRE (lanes 5 to 8) or a DR-1 HRE in which a single half-site had been mutated (lanes 1 to 4). Amounts of partially purified RXR DBD used were 12.5 ng (lanes 1 and 5), 37.5 ng (lanes 2 and 6), 113 ng (lanes 3 and 7), and 340 ng (lanes 4 and 8). Positions of monomeric and dimeric RXR DBD complexes with DNA are indicated. (**B**) Gel mobility-shift assays were done with 340 ng of partially purified RXR DBD 130–223 and ^{32}P-labeled oligonucleotides containing two AGGTCA half-sites separated by a spacer ranging from zero to five nucleotides in length (DR-0 through DR-5) as indicated. Positions of the monomeric and dimeric RXR DBD complexes with DNA are shown.

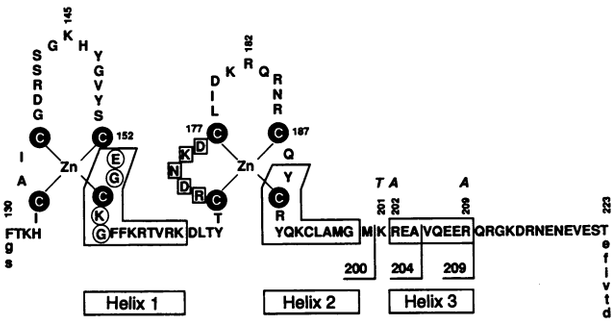

Fig. 1. Schematic representation of the 94-residue segment (Phe^{130} to Thr^{223}) of the human RXRα DBD used in this study (28). The locations of the three helices determined from the NMR data are indicated by boxes. Circled residues indicate amino acids essential for discrimination between glucocorticoid and estrogen half-site sequences (P box). Individually boxed residues indicate amino acids (172 to 176) responsible for protein-protein interactions in the dimeric GR-DNA complex (D box). Truncation points for derivatives 130–209, 130–204, and 130–200 are indicated by vertical lines. Amino acid substitutions in mutants K201T,R202A and R209A are indicated above the sequence. Flanking residues from the expression vector are shown in lowercase letters.

bind cooperatively as a dimer to the DR-1 HRE (Fig. 4A). However, further truncation to Ala[204] (RXR DBD 130–204), disrupting the third helix, resulted in changes in binding properties (*22*). In contrast to RXR DBD 130–209, which binds almost exclusively as a dimer at all concentrations tested, RXR DBD 130–204 binds predominantly as a monomer at lower protein concentrations (Fig. 4A). These data establish a role for the third helix in mediating the protein-protein interactions necessary for cooperative binding of the RXR DBD to an HRE. A final truncation construct that deleted residues beyond Met[200] (RXR DBD 130–200) failed to bind DNA as either a monomer or dimer (Fig. 4A). Thus, the third helix of the RXR DBD facilitates both DNA-protein and protein-protein interactions required for high-affinity binding of the RXR DBD to its cognate HRE. Our results are consistent with a recent study of chimeras between RXRβ and the orphan receptor NGFI-B in which a 12–amino acid region of the RXRβ DBD, which includes the third helix in the RXRα DBD, was implicated in specifying RXR binding activity (*23*).

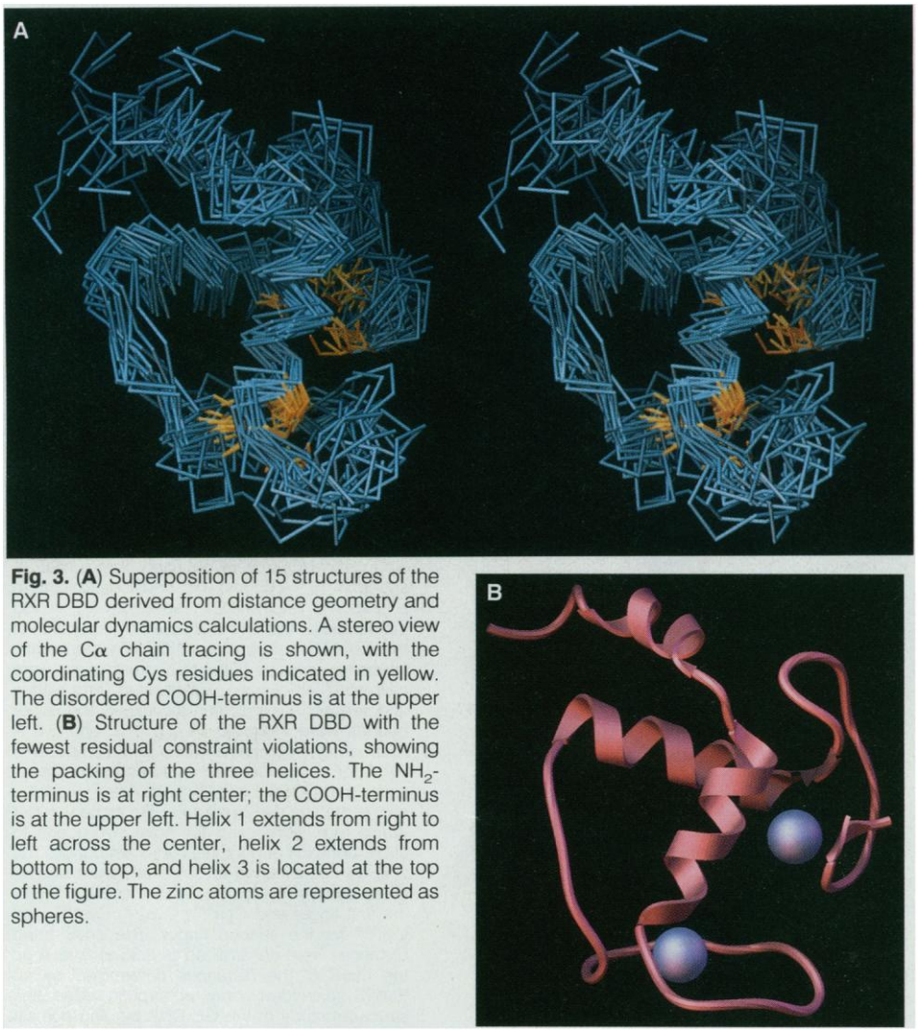

Fig. 3. (**A**) Superposition of 15 structures of the RXR DBD derived from distance geometry and molecular dynamics calculations. A stereo view of the Cα chain tracing is shown, with the coordinating Cys residues indicated in yellow. The disordered COOH-terminus is at the upper left. (**B**) Structure of the RXR DBD with the fewest residual constraint violations, showing the packing of the three helices. The NH_2-terminus is at right center; the COOH-terminus is at the upper left. Helix 1 extends from right to left across the center, helix 2 extends from bottom to top, and helix 3 is located at the top of the figure. The zinc atoms are represented as spheres.

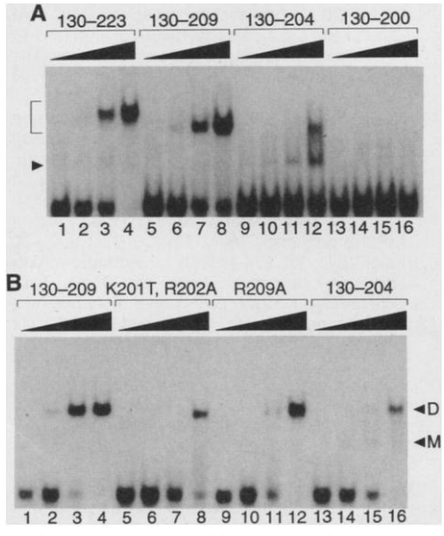

Fig. 4. Helix 3 mediates DNA-protein and protein-protein interactions required for cooperative binding of the RXR DBD to a DR-1 HRE. (**A**) Gel mobility-shift assays used progressively increasing amounts of RXR DBD 130–223 and truncation derivatives 130–209, 130–204, and 130–200 and ^{32}P-labeled oligonucleotide encoding a DR-1 HRE. Positions of the monomeric (arrowhead) and dimeric (bracket) RXR DBD complexes with DNA are indicated on the left. Amounts of partially purified RXR DBD derivatives used were 12.5 ng (lanes 1, 5, 9, and 13), 37.5 ng (lanes 2, 6, 10, and 14), 113 ng (lanes 3, 7, 11, and 15), and 340 ng (lanes 4, 8, 12, and 16). (**B**) Gel mobility-shift assays were done with increasing amounts of RXR DBD 130–209, RXR DBD 130–204, point mutants K201T,R202A and R209A, and ^{32}P-labeled oligonucleotide encoding a DR-1 HRE. Positions of the monomeric (M) and dimeric (D) RXR DBD complexes with DNA are indicated on the right. Amounts of partially purified RXR DBD proteins used were 37 ng (lanes 1, 5, 9, and 13), 111 ng (lanes 2, 6, 10, and 14), 333 ng (lanes 3, 7, 11, and 15), and 1000 ng (lanes 4, 8, 12, and 16).

To test the prediction from modeling that basic residues located on either end of the third helix (Lys[201], Arg[202], and Arg[209]) interact with the phosphate backbone across the minor groove, we generated RXR DBD mutants (*24*) that contained alterations of either Lys[201] and Arg[202] [Lys[201] and Arg[202] mutated to Thr and Ala, respectively (K201T,R202A)] or Arg[209] [Arg[209] mutated to Ala (R209A)]. In gel mobility-shift assays, K201T,R202A and R209A bound approximately seven- and threefold less efficiently, respectively, to the DR-1 HRE relative to the wild-type protein RXR

DBD 130–209 (Fig. 4B). These data support the prediction that basic amino acids on either end of the third helix may directly interact with DNA. We note that although both mutants K201T,R202A and R209A displayed reduced overall binding affinities, they retained the ability to bind cooperatively as dimers (Fig. 4B). Thus, the dimerization and DNA binding activities of the third helix appear to be separable functions.

We have identified a helical region in the RXR DBD that provides external surfaces for two additional functions. First, this third helix positions basic amino acids required for high-affinity interactions with DNA. Second, it serves as a dimerization interface for interactions between RXR molecules. Identification of this additional helix thus provides insight into the structural features that underlie receptor binding to direct repeat HREs. Interestingly, the eight amino acids that comprise the third helix are conserved in the isoforms of the RXR identified in human, mouse, and *Xenopus laevis* (*25*) as well as in Ultraspiracle (Usp), the *Drosophila melanogaster* homolog of the RXR (*26*). The Usp protein, like the RXR, preferentially binds as a homodimer to a DR-1 HRE and can form heterodimers with the mammalian PPAR, VDR, TR, and RAR as well as with the *Drosophila* ecdysone receptor (*27*). This strict conservation suggests that the third helix in the RXR DBD functions not only in RXR homodimerization but may function in the interaction of RXR-Usp with other members of the nuclear hormone receptor superfamily.

REFERENCES AND NOTES

1. R. M. Evans, *Science* **240**, 889 (1988).
2. K. Umesono *et al.*, *Cell* **65**, 1255 (1991).
3. D. J. Mangelsdorf, E. S. Ong, J. A. Dyck, R. M. Evans, *Nature* **345**, 224 (1990); S. A. Kliewer, K. Umesono, D. J. Mangelsdorf, R. M. Evans, *ibid.* **355**, 446 (1992); X.-k. Zhang, B. Hoffmann, P. B.-V. Tran, G. Graupner, M. Pfahl, *ibid.*, p. 441; V. C. Yu *et al.*, *Cell* **67**, 1251 (1991); M. Leid *et al.*, *ibid.* **68**, 377 (1992); M. S. Marks *et al.*, *EMBO J.* **11**, 1419 (1992); T. H. Bugge, J. Pohl, O. Lonnoy, H. G. Stunnenberg, *ibid.*, p. 1409.
4. S. A. Kliewer *et al.*, *Nature* **358**, 771 (1992).
5. D. J. Mangelsdorf *et al.*, *Cell* **66**, 555 (1991); A. A. Levin *et al.*, *Nature* **355**, 359 (1992); R. A. Heyman *et al.*, *Cell* **68**, 397 (1992); X.-k. Zhang *et al.*, *Nature* **358**, 587 (1992).
6. S. A. Kliewer *et al.*, *Proc. Natl. Acad. Sci. U.S.A.* **89**, 1448 (1992).
7. RXR DBD 130–223 was expressed as a fusion protein with glutathione-S-transferase (GST) with the pGEX-2T expression vector (Pharmacia). The polymerase chain reaction (PCR) was used to produce a DNA sequence encoding residues 130 to 223 of the RXR containing an in-frame Bam HI site and an Eco RI site. The fragment generated by PCR was confirmed by sequencing BL21-(DE3)plysS cells containing the pGEX-2T–RXR DBD 130–223 expression vector were typically grown in Luria broth. However, ^{15}N-labeled RXR DBD 130–223 samples were grown in minimal media [44 mM Na_2HPO_4, 22 mM KH_2PO_4, 9 mM NaCl, 1 mM $MgSO_4$, 0.1 μM $CaCl_2$, 0.02 μM $FeCl_3$, 1% glucose, and thiamine (1 mg/liter)] containing 1 g/liter [$(^{15}NH_4)_2SO_4$] (Cambridge Isotope Laboratories, Woburn, MA). Cells were grown to an absorbance at 600 nm of approximately 0.8, fusion protein expression was induced for 3 hours with 0.5 mM isopropyl-β-D-thiogalactopyranoside, and the pelleted cells were resuspended and lysed by freeze-thawing in buffer containing 50 mM tris (pH 8.0), 250 mM KCl, 5 μM $ZnCl_2$, 1 mM dithiothreitol (DTT), 1 mM phenylmethylsulfonyl fluoride (PMSF), and 1% Triton X-100. Lysates were clarified by centrifugation for 1 hour at 45,000*g* in a Ti60 (Beckman) rotor. Glutathione-Sepharose beads (Pharmacia) were added to the crude bacterial lysates containing the GST–RXR DBD 130–223 protein, and the fusion protein–glutathione-Sepharose complexes were then pelleted and washed three times in phosphate-buffered saline containing 1 mM DTT. The fusion protein was eluted from the glutathione-Sepharose beads and the GST cleaved from RXR DBD 130–223 with thrombin (Sigma) in buffer containing 50 mM tris (pH 8.0), 2.5 mM $CaCl_2$, 1 mM DTT, and 5 mM glutathione. The eluted protein was loaded onto a heparin-agarose column and then washed with buffer A [20 mM tris (pH 8.0), 1 mM DTT, and 1 mM PMSF] containing 100 mM KCl. The RXR DBD 130–223 was eluted with a linear salt gradient extending from 100 mM to 800 mM KCl. The purified protein was used for the NMR studies. The oligonucleotides used for PCR of RXR DBD 130–223 were TATGGATCCT-TCACCAAGCACATCTGCGCC (sense) and TAT-GAATTCGGTCGACTCCACCTCATTCTC (antisense).
8. Gel mobility-shift assays (20 μl) contained 10 mM tris (pH 8.0), 0.1% NP-40, 6% glycerol, 1 mM DTT, 1 μg of polydeoxyinosine-polydeoxycytosine, and RXR DBD 130–223. After a 10-min incubation on ice, 1 ng of ^{32}P-labeled oligonucleotide was added and the incubations continued for an additional 10 min. DNA protein complexes were resolved on a 6% polyacrylamide gel in 0.25× TBE [1× TBE = 90 mM tris (pH 8.0), 90 mM boric acid, and 2 mM EDTA]. Gels were dried and subjected to autoradiography at −70°C. The oligonucleotides and their compliments used in the gel mobility-shift assays were TCGACGACCAGGTCAAAGGT-CACGTTCTAG (DR-1) and TCGACGACCAGGT-CAAGAACTGCGTTCTAG (ΔDR-1; half-site).
9. T. Härd *et al.*, *Science* **249**, 157 (1990); T. Hard *et al.*, *Biochemistry* **29**, 9015 (1990).
10. J. W. R. Schwabe, D. Neuhaus, D. Rhodes, *Nature* **348**, 458 (1990).
11. M. Katahira *et al.*, *Biochemistry* **31**, 6474 (1992).
12. Samples for NMR experiments, typically 0.5 to 1.0 mM, were prepared in 95% ^1H_2O and 5% ^2H_2O or in 100% ^2H_2O with a Pharmacia flow cell. The samples were concentrated against buffer containing 20 mM potassium phosphate, 100 mM KCl, 50 μM $ZnCl_2$, and 10 mM DTT at pH 6.7 to 6.9. All solvents were purged with argon gas. The presence of DTT in the NMR sample is essential to prevent oxidation of the cysteines.
13. NMR experiments were performed at 7°, 17°, and 27°C with Bruker (Karlsruhe, Germany) AMX-600 and AM-600 spectrometers. The 2D total correlation spectroscopy (TOCSY) experiments were performed according to the method of Rance [M. Rance, *J. Magn. Reson.* **74**, 557 (1987)] with a DIPSI-2 sequence [A. J. Shaka, C. J. Lee, A. Pines, *ibid.* **77**, 274 (1988)] for isotropic mixing and spin-lock periods of 30 or 40 ms. Two-dimensional nuclear Overhauser enhancement spectroscopy (NOESY) spectra with mixing times (τ_m) of 60, 100, and 200 ms were recorded with the standard pulse sequence followed by a short Hahn-echo period to improve the quality of the base line [M. Rance and R. A. Byrd, *ibid.* **54**, 221 (1983)]. Two-dimensional jump and return NOESY spectra with 100-, 150-, and 200-ms mixing times were also recorded [A. Bax, V. Sklenar, G. M. Clore, A. M. Gronenborn, *J. Am. Chem. Soc.* **109**, 7188 (1987)]. Spectra were usually acquired with 4096 complex data points with a spectral width in the F_2 dimension of 12.5 kHz, an F_1 spectral width of approximately 7 kHz, and 512 increments in the time period t_1 with 128 scans per t_1 value. A 2D ^1H–^{15}N correlated spectrum (HSQC) was acquired with standard methods [A. Bax, M. Ikura, L. E. Kay, D. A. Torchia, R. Tschudin, *J. Magn. Reson.* **86**, 304 (1990); T. J. Norwood, J. Boyd, J. E. Heritage, N. Soffe, I. D. Campbell, *ibid.* **87**, 488 (1990)]. A heteronuclear 3D TOCSY-HSQC spectrum with a spin-lock period of 40 ms and a NOESY-HSQC spectrum with mixing time of 100 ms were recorded consecutively in order to minimize differences in sample conditions. The 3D experiments were acquired with 256 increments in the time period t_3, 16 scans per t_3 value, 256 t_3 increments, and 64 increments in the time period t_2 (the ^{15}N dimension). All 2D data were processed on a Convex C240 computer with a modified version of the FTNMR software (Hare Research, Woodinville, WA). For all experiments in 95% ^1H_2O and 5% ^2H_2O, a low-pass filter was applied to the time domain data before Fourier transformation to suppress the solvent signal [D. Marion, M. Ikura, A. Bax, *ibid.* **84**, 425 (1989)]. The 3D data were processed with a modified version of FTNMR for the F_1-F_3 planes and a separate routine written by M. Rance (The Scripps Research Institute) for the F_2 Fourier transform.
14. B. F. Luisi *et al.*, *Nature* **352**, 497 (1991).
15. In structures calculated for the full, 94-residue protein, the NH_2- and COOH-terminal residues are highly disordered.
16. The NOEs involving backbone amide protons were obtained from a 3D ^1H–^{15}N NOESY-HSQC spectrum (τ_m = 100 ms). Long-range side chain–side chain NOEs were obtained from a NOESY spectrum (τ_m = 60 ms) with additional data from a jump and return NOESY spectrum (τ_m = 100 ms) for the protons most affected by irradiation of the water. For each of the NOESY experiments, integrated volumes of the NOE cross peaks were calibrated empirically with known intraresidue and sequential interproton distances. The upper bounds were assigned as 2.5, 3.5, and 5.0 Å for backbone-backbone NOEs and 3.0, 4.0, and 5.0 Å for backbone–side chain and side chain–side chain NOEs. Lower bounds were set to the sum of the van der Waals radii. Reduced van der Waals radii were used for polar hydrogens to allow formation of potential hydrogen bonds. The zinc was constrained to be tetrahedrally coordinated by Cys^{135}, Cys^{138}, Cys^{152}, and Cys^{155} for the first finger and Cys^{171}, Cys^{177}, Cys^{187}, and Cys^{190} for the second finger. The Zn–S bond distances were constrained to 2.35 ± 0.05 Å on the basis of the distances determined by an EXAFS (extended x-ray absorption edge fine structure) study of the GR DNA binding domain [L. P. Freedman *et al.*, *Nature* **334**, 543 (1988)], and the bond angles were constrained to 109 ± 10°.
17. T. F. Havel and K. Wüthrich, *Bull. Math. Biol.* **46**, 673 (1984).
18. Pseudoatoms were used wherever necessary [K. Wüthrich, M. Billeter, W. Braun, *J. Mol. Biol.* **169**, 949 (1983)]. In addition to the NOE constraints, explicit backbone amide-carbonyl hydrogen bonds and φ angle constraints were enforced in the helical regions during the DISGEO calculations. The regions of helical secondary structure were identified from the extensive networks of medium-range NOEs ($C\alpha H_i$–$C\beta H_{i+3}$ and $C\alpha H_i$–$NH_{i+3,i+4}$). These hydrogen bond and φ angle constraints were used only in the DISGEO calculations to ensure formation of correctly folded right-handed helices; they were omitted from the subsequent restrained molecular dynamics calculations. In the absence of these helix-forcing constraints, DISGEO tends to produce structures with incorrectly folded helices that violate the medium-range NMR constraints [H. J. Dyson, G. P. Gippert, D. A. Case, A. Holmgren, P. E. Wright, *Biochemistry* **29**, 4129 (1990)].
19. M. S. Lee, G. P. Gippert, K. V. Soman, D. A. Case, P. E. Wright, *Science* **245**, 635 (1989).
20. S. J. Weiner, P. A. Kollman, D. T. Nguyen, D. A. Case, *J. Comput. Chem.* **7**, 230 (1986).
21. RXR DBD constructs 130–209, 130–204, and 130–

200 were generated by PCR and expressed as fusion proteins with GST, and the proteins were purified on glutathione-sepharose and clipped with thrombin as described above. The antisense oligonucleotides used for PCR were TATGAATTC-TCACCGCTCCTCCTGCACGGCTTC (130–209); TATGAATTCTCAGGCTTCCCGCTTCATGCCCAT (30–204); TATGAATTCTCACATGCCCATGGCCA-GGCACTT (130–200).
22. RXR DBD 130–204 was folded correctly as determined by 2D NMR analysis (M. S. Lee and P. E. Wright, unpublished results).
23. T. E. Wilson, R. E. Paulsen, K. A. Padgett, J. Milbrandt, *Science* **256**, 107 (1992). When placed into the equivalent region of NGFI-B, the 12–amino acid segment from RXRβ blocks binding to the NGFI-B recognition sequence (5′-AAAG-GTCA-3′) and promotes binding to a DR-1–type motif (other spacing options were not examined). These data are consistent with a potential role for this region in dimer formation.
24. RXR DBD mutants K201T,R202A and R209A were generated by PCR and expressed as fusion proteins with GST, and the proteins were purified on glutathione-sepharose and clipped with thrombin as described above. The antisense oligonucleotides used for PCR were TATGAATTCTCACCGCTCCTC-CTGCACGGCTTCCGCCGTCATGCCCAT (K201T, R202A) and TATGAATTCTCACGCCTCCTCCTGC-ACGGCTTCCCG (R209A).
25. D. J. Mangelsdorf *et al.*, *Genes Dev.* **6**, 329 (1992); B. Blumberg *et al.*, *Proc. Natl. Acad. Sci. U.S.A.* **89**, 2321 (1992).
26. A. E. Oro *et al.*, *Nature* **347**, 298 (1990).
27. T.-P. Yao *et al.*, *Cell* **71**, 63 (1992); T.-P. Yao and R. M. Evans, unpublished results.
28. Abbreviations for the amino acid residues are: A, Ala; C, Cys; D, Asp; E, Glu; F, Phe; G, Gly; H, His; I, Ile; K, Lys; L, Leu; M, Met; N, Asn; P, Pro; Q, Gln; R, Arg; S, Ser; T, Thr; V, Val; W, Trp; and Y, Tyr.
29. We thank M. Pique for assistance with computer graphics and U. Genick, D. Sem, G. Gippert, D. Case, K. Umesono, T. Perlmann, D. Mangelsdorf, and J. Zhou for discussion. This work was supported by the Jane Coffin Childs Memorial Fund for Medical Research (S.A.K.), NIH (P.E.W. and R.M.E.), the National Cancer Institute (R.M.E.), and a computing grant from Cray Research (P.E.W.). R.M.E. is an Investigator of the Howard Hughes Medical Institute at the Salk Institute for Biological Studies.

13 January 1993; accepted 31 March 1993

Generation of Allospecific Natural Killer Cells by Stimulation Across a Polymorphism of HLA-C

Marco Colonna, Edward G. Brooks, Michela Falco, Giovan Battista Ferrara, Jack L. Strominger

The cytotoxicity of human natural killer (NK) cells is modulated by the major histocompatibility complex human leukocyte antigen (HLA)–C molecules on the surface of the target cell. Alloreactive NK cells specific for the NK-1 alloantigen could be reproducibly generated from individuals that were homozygous for HLA-C with asparagine at residue 77 and lysine at residue 80 [HLA-C(Asn^{77}, Lys^{80})] by stimulation with target cells that were homozygous for HLA-C(Ser^{77}, Asn^{80}); the reciprocal stimulation yielded NK cells specific for the NK-2 alloantigen. However, neither homozygous target cell stimulated the generation of alloreactive NK cells from heterozygous individuals. Thus, these data reveal an unanticipated difference between human NK alloreactivity defined by this system and murine "hybrid resistance."

Natural killer cells make up a subpopulation of about 10 to 15% of peripheral blood lymphocytes (PBLs) that lyse tumor and virus-infected cells independently of antigen presentation by the major histocompatibility complex (MHC) molecules (*1*). Some NK cells can specifically recognize and lyse normal allogeneic cells (*2*, *3*). The alloantigen NK-1 on target cells is controlled by HLA-C or by a closely linked gene (*4*–*6*). Target cells that are susceptible to allospecific lysis are homozygous for a two–amino acid polymorphism of HLA-C, namely, Ser^{77} and Asn^{80} [HLA-C(Ser^{77}, Asn^{80})] in the α1 domain (shared by HLA-Cw1, -Cw3, -Cw7, -Cw8, and by some of the -Cw blank alleles). In addition, a second alloantigen (NK-2) correlates with homozygosity for a different pair of amino acids at the same positions [HLA-C(Asn^{77}, Lys^{80})] (shared by HLA-Cw2, -Cw4, -Cw5, -Cw6, and some other -Cw blank alleles). Cells heterozygous for these pairs of amino acids cannot be lysed by NK clones that recognize NK-1 or NK-2.

The requirement for both HLA-C alleles of the target to be of the same type for lysis by a given NK clone to occur (recessive susceptibility) implicates the alternative HLA-C allele as having an inhibitory function on that NK clone (dominant suppression). It also provides a rationale for the reproducible generation of NK cells with NK-1 and NK-2 allospecificities that have so far only been generated by stimulation between random donors. Assuming a reciprocal inhibitory function for the two types of alleles of HLA-C, NK cell lines that specifically recognize cells homozygous for HLA-C(Ser^{77}, Asn^{80}) or for HLA-C (Asn^{77}, Lys^{80}) should be reproducibly established by reciprocal stimulation between cells homozygous for the alternative polymorphisms.

Individuals chosen at random (n = 28) were DNA typed for residues 77 and 80 of HLA-C with sequence-specific oligonucleotides; 12 were homozygous for HLA-C(Ser^{77}, Asn^{80}) (42.9%), 4 were homozygous for HLA-C(Asn^{77}, Lys^{80}) (14.3%), and 12 were heterozygous (42.9%) (Table 1). In the homozygotes Ser^{77} was always linked to Asn^{80}, and Asn^{77} to Lys^{80}, in agreement with the known HLA-C sequences (Fig. 1) (*7*). To generate an NK cell line with specificity for NK-1, we purified CD3$^-$, CD4$^-$, CD8$^-$ lymphocytes from the PBLs of an HLA-C(Asn^{77}, Lys^{80}) homozygous donor (EB) by complement-mediated depletion and cocultured the lymphocytes with γ-irradiated PBLs from an HLA-C(Ser^{77}, Asn^{80}) homozygous donor (HD). After 3 days, interleukin-2 (IL-2) was added to the culture medium, and CD3$^-$, CD4$^-$, CD8$^-$ lymphocytes were expanded four to five times in a 7-day

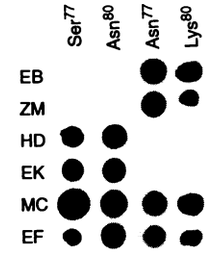

Fig. 1. Oligonucleotide typing of residues 77 and 80 of HLA-C in the blood donors from whom the NK cell lines were derived. Genomic DNA was extracted from PBLs by standard techniques. The second exon of HLA-C was selectively amplified from genomic DNAs by PCR. Primer pairs and reaction conditions for the amplification were previously described (*6*). Amplified fragments were denatured in 0.4 N NaOH and applied to Hybond-N (Amersham) with a slot blot apparatus (Schleicher & Schuell, Inc.). Membranes were hybridized with ^{32}P-labeled oligonucleotides specific for Ser^{77} or Asp^{77} (*6*) and oligonucleotides [CCTGCGGAA(A or C)CTGCGC-GGC] (nucleotides 303 to 321) specific for Asp^{80} or Lys^{80}, respectively. Hybridization was carried out for 2 hours at 42°C in 5× Denhardt's solution, 5× standard saline phosphate–EDTA [SSPE; 1× SSPE contains 0.18 M NaCl, 10 mM phosphate (pH 7.4), and 1 mM EDTA] plus 0.5% SDS, and probe at 2 × 10^6 cpm/ml. Membranes were washed in 6× standard saline citrate (SSC)–0.1% SDS for 10 min at room temperature and for 10 min at the calculated t_m (melting temperature) for each oligonucleotide. Similar data were obtained for each of the target cells shown in Table 1.

M. Colonna, Laboratory of Immunogenetics, Istituto Nazionale per la Ricerca sul Cancro, 16132 Genoa, Italy, and Department of Biochemistry and Molecular Biology, Harvard University, Cambridge, MA 02138.
E. G. Brooks, Division of Tumor Virology, Dana-Farber Cancer Institute, Harvard Medical School, Boston, MA 02115.
M. Falco and G. B. Ferrara, Laboratory of Immunogenetics, Istituto Nazionale per la Ricerca sul Cancro, 16132 Genoa, Italy, and Centro Ricerche A.V.I.S., Bergamo, Italy.
J. L. Strominger, Department of Biochemistry and Molecular Biology, Harvard University, Cambridge, MA 02138, and Division of Tumor Virology, Dana-Farber Cancer Institute, Harvard Medical School, Boston, MA 02115.